

# Properties of Color-Coulomb String Tension

Y. Nakagawa,<sup>1</sup> A. Nakamura,<sup>2</sup> T. Saito,<sup>1</sup> H. Toki,<sup>1</sup> and D. Zwanziger<sup>3</sup>

<sup>1</sup>*Research Center for Nuclear Physics,*

*Osaka University, Ibaraki, Osaka 567-0047, Japan*

<sup>2</sup>*Research Institute for Information Science and Education,*

*Hiroshima University, Higashi-Hiroshima 739-8521, Japan*

<sup>3</sup>*Physics Department, New York University, New York, NY 10003, USA*

## Abstract

We study the properties of the color-Coulomb string tension obtained from the instantaneous part of gluon propagators in Coulomb gauge using quenched  $SU(3)$  lattice simulation. In the confinement phase, the dependence of the color-Coulomb string tension on the QCD coupling constant is smaller than that of the Wilson loop string tension. On the other hand, in the deconfinement phase, the color-Coulomb string tension does not vanish even for  $T/T_c = 1 \sim 5$ , the temperature dependence of which is comparable with the magnetic scaling, dominating the high temperature QCD. Thus, the color-Coulomb string tension is not an order parameter of QGP phase transition.

PACS numbers: 12.38.Aw, 12.38.Gc, 11.15.Ha

Keywords: lattice QCD, color confinement, Coulomb gauge, quark-gluon plasma

## I. INTRODUCTION

Understanding color confinement in quantum chromodynamics (QCD) is one of the most challenging problems in quantum field theory, and also provides essential knowledge for low temperature hadron physics. There are many approaches to understand color confinement dynamics: dual superconductor scenario, center vortex model, the infrared behavior of gluon propagators, etc. have been widely studied and a large amount of information on color confinement has been accumulated. See reviews in Refs. [1, 2, 3]. In those scenarios, topological objects and gauge-dependent quantities, bringing out the properties of QCD vacuum, may play an important role. A key issue is the choice of gauge in which the confinement scenario is realized.

Recently, there has been considerable interest in the Coulomb gauge color confinement scenario. This scenario was originally discussed by Gribov [4], and in recent years, Zwanziger has advocated the importance of a color-Coulomb potential in Coulomb gauge for color confinement [5]. He and his collaborators showed that, in Coulomb gauge, the time-time component of gluon propagators,  $g^2 D_{00}$ , including an instantaneous color-Coulomb potential plus a noninstantaneous vacuum polarization, is invariant under renormalization [5, 6, 7]. It has been found by perturbative analysis [7] that the instantaneous part in Coulomb gauge QCD causes antiscreening, while the vacuum polarization part causes screening. Hence, one expects that the instantaneous color-Coulomb potential represents a linearly rising behavior for large quark separations. Moreover, Zwanziger pointed out that there is an inequality [10],  $V_{phys}(R) \leq V_{coul}(R)$ , where  $V_{phys}(R)$  means a physical heavy-quark-antiquark potential and  $V_{coul}(R)$  the Coulomb heavy-quark potential corresponding to the instantaneous part of  $D_{00}$ . This inequality indicates that if the physical heavy-quark potential is confining, then the Coulomb heavy-quark potential is also confining. See Ref. [8] for a review.

In order to verify the Coulomb gauge color confinement scenario, one needs a nonperturbative technique to describe the low-energy color confinement. Therefore, nonperturbative verifications have been tried in lattice gauge simulation. In the  $SU(2)$  lattice numerical simulation carried out by Cucchieri and Zwanziger [9], it was found that  $g^2 D_{00}(\vec{k})$  is strongly enhanced at  $\vec{k} = 0$ . In  $SU(2)$  and  $SU(3)$  lattice simulations [11, 12, 13], furthermore, it was reported that the Coulomb heavy-quark potential grows linearly at large quark separations in the confinement phase.

On the lattice, it is essential to study the magnitude and the scaling for the string tension, which is a characteristic quantity for confinement physics. Numerical lattice calculations [11, 12, 13] indicate that the color-Coulomb string tension has 2 – 3 times larger value in comparison with the case of a gauge invariant Wilson loop, as expected by  $V_{phys}(R) \leq V_{coul}(R)$ . In addition, the  $SU(2)$  lattice numerical data in Ref. [12] show the possibility that an asymptotic scaling violation for the color-Coulomb string tension may be less than the usual Wilson loop string tension. Accordingly, the dependence of the color-Coulomb string tension on a gauge coupling or a lattice cutoff ought to be extensively investigated in  $SU(3)$  lattice gauge theory.

The lattice simulations mentioned above have shown the linearity of the instantaneous color-Coulomb potential at large distances in the confinement regions. At the same time, the lattice calculations at finite temperature in the deconfinement phase indicate that the Coulomb string tension remains after the quark-gluon plasma (QGP) phase transition [12, 13]. One possible explanation is that the color-Coulomb potential, determined by the spatial-like and time (temperature) independent Faddeev-Popov operator, is not sensitive to the system temperature. In addition, we note that the potential obtained from a spatial Wilson loop above  $T_c$  behaves as a linearly rising function [17, 18, 19, 20, 21, 22, 23, 24]. Both the color-Coulomb and the spatial Wilson potentials have a common feature that they are defined by spatial variables. However, the higher temperature lattice simulations than the previous calculations [12, 13] are indispensable. Nevertheless, the noninstantaneous retarded part with the vacuum polarization still gives a color-screened potential [13, 25, 26].

In Coulomb gauge QCD there are no unphysical degrees of freedom for gauge fields; namely, Coulomb gauge is a physical gauge. In contrast, Lorentz covariant gauges generate a negative spectral function due to the indefinite metric of Fock space. This is very convenient on discussing a physical hadron, and a lot of attempts have been made to construct models based on the Coulomb gauge Hamiltonian to describe color confinement [27, 28, 29, 30, 31] and hadrons [32, 33].

In this paper, we will perform more extensive lattice QCD studies on the Coulomb gauge confinement scenario comparing with the previous calculation [13]. In the confinement phase, we investigate the scaling behavior of the color-Coulomb string tension by varying a lattice cutoff or a coupling constant  $\beta = 6/g^2$ . In the deconfinement phase, we discuss the relation between the thermal color-Coulomb string tensions, which are calculated at high

temperatures,  $T/T_c = 1.5 \sim 5.0$ , and the magnetic scaling that is believed to dominate the high temperature QCD. In Sec. II we briefly review the partition function in Coulomb gauge and describe the instantaneous color-Coulomb potential and the noninstantaneous vacuum polarization part. In Sec. III, we give the definition of the partial-length Polyakov line correlator[11, 12] to evaluate the instantaneous part. Section IV is devoted to show the numerical results. Section V gives conclusions.

## II. INSTANTANEOUS COLOR-COULOMB POTENTIAL

The construction of the partition function in Coulomb gauge through the Faddeev-Popov technique and the derivation of the instantaneous color-Coulomb potential were done in Ref. [6]. The Hamiltonian of QCD in Coulomb gauge can be written as

$$H = \frac{1}{2} \int d^3x (E_i^{tr2}(\vec{x}) + B_i^2(\vec{x})) + \frac{1}{2} \int d^3x d^3y (\rho(\vec{x}) \mathcal{V}(\vec{x}, \vec{y}) \rho(\vec{y})), \quad (1)$$

where  $E_i^{tr}$ ,  $B_i$  and  $\rho$  are the transverse electric field, the magnetic field and the color charge density, respectively. The function  $\mathcal{V}$  in the second term is made by the Faddeev-Popov (FP) operator in the spatial direction,  $M = -\vec{D}\vec{\partial} = -(\vec{\partial}^2 + g\vec{A} \times \vec{\partial})$ ,

$$\mathcal{V}(\vec{x}, \vec{y}) = \int d^3z \left[ \frac{1}{M(\vec{x}, \vec{z})} (-\vec{\partial}_{(\vec{z})}^2) \frac{1}{M(\vec{z}, \vec{y})} \right]. \quad (2)$$

From the partition function with Hamiltonian Eq. (1), one can evaluate the time-time gluon propagator composed of the following two parts:

$$g^2 \langle A_0(x) A_0(y) \rangle = g^2 D_{00}(x - y) = V(x - y) + P(x - y), \quad (3)$$

where

$$V(x - y) = g^2 \langle \mathcal{V}(\vec{x}, \vec{y}) \rangle \delta(x_4 - y_4). \quad (4)$$

The equation (4) corresponds to the instantaneous color-Coulomb potential at equal time and causes antiscreening; namely, it is the most important quantity in Coulomb gauge confinement scenario, and is constructed by the spatial FP matrix. Therefore, if the potential  $V$  is a linearly rising potential for large quark separations, then color confinement is attributed to an enhancement of the low-lying mode of FP eigenvalues [4, 5]. Note that Eq. (4) in the case of quantum electrodynamics (QED) as a non-confining theory is identified as a

Coulomb propagator  $\langle -1/\partial_i^2 \rangle$  or a Coulomb potential  $1/r$ . Simultaneously, the quantity  $P$  in Eq. (3) is a vacuum polarization term,

$$P(x-y) = -g^2 \langle \int \mathcal{V}(\vec{x}, \vec{z}) \rho(\vec{z}, x_4) d^3 z \int \mathcal{V}(\vec{y}, \vec{z}') \rho(\vec{z}', y_4) d^3 z' \rangle, \quad (5)$$

which causes color-screening effect owing to the minus sign of this equation, and produces the reduction of a color-confining force and a quark-pair creation from vacuum when dynamical quarks exist. Moreover, this perturbative argument is also satisfied at one-loop order [5].

### III. PARTIAL-LENGTH POLYAKOV LINE

In this section, we give the definition of a static heavy quark-antiquark potential in the color-singlet channel as a function of distance,  $R$ , and summarize how to fix the gauge on the lattice.

We introduce a partial-length Polyakov line (PPL) defined as [11, 12]

$$L(\vec{x}, n_t) = \prod_{n_s=1}^{n_t} U_0(\vec{x}, n_s), \quad n_t = 1, 2, \dots, L_t. \quad (6)$$

Here  $U_0(\vec{x}, t) = \exp(iagA_0(\vec{x}, t))$  is an  $SU(3)$  link variable in the temporal direction and  $a$ ,  $g$ ,  $A_0(\vec{x}, t)$  and  $L_t$  represent the lattice cutoff, the gauge coupling, the time component of gauge potential and the temporal-lattice size. A PPL correlator in color-singlet channel is given by

$$G(R, n_t) = \frac{1}{3} \langle \text{Tr}[L(R, n_t)L^\dagger(0, n_t)] \rangle, \quad (7)$$

where  $R$  stands for  $|\vec{x}|$ . From Eq. (7) one evaluates the color-singlet potential on the lattice,

$$V(R, n_t) = \log \left[ \frac{G(R, n_t)}{G(R, n_t + 1)} \right]. \quad (8)$$

In the case of  $n_t = 0$ , we define

$$V(R, 0) = -\log[G(R, 1)]. \quad (9)$$

Greensite et al. argued that this function  $V(R, 0)$  in Coulomb gauge corresponds to an instantaneous color-Coulomb potential  $V_{coul}(R)$  [11, 12]. The potential  $V(R, n_t)$  in the limit  $n_t \rightarrow \infty$  is expected to correspond to a physical potential,  $V_{phys}(R)$ , usually calculated from the Wilson loops in the same limit. Both potentials are known to satisfy Zwanziger's inequality,  $V_{phys}(R) \leq V_{coul}(R)$  [10].

Since the color-decomposed potential defined by the PPL correlator such as Eq. (7), do not have a gauge invariant form, we must fix the gauge. One can realize the Coulomb gauge on the lattice to maximize the measurement

$$\sum_{\vec{x}} \sum_{i=1}^3 \text{ReTr} U_i^\dagger(\vec{x}, t), \quad (10)$$

by repeating the gauge rotations:

$$U_i(\vec{x}, t) \rightarrow U_i^\omega(\vec{x}, t) = \omega^\dagger(\vec{x}, t) U_i(\vec{x}, t) \omega(\vec{x} + \hat{i}, t), \quad (11)$$

where  $\omega \in SU(3)$  [46] is a gauge rotation matrix and  $U_i(\vec{x}, t)$  are link variables for the spatial direction. Thus, each lattice configuration thermalized after the Monte Carlo quantization can be gauge fixed iteratively [34].

#### IV. RESULTS AND DISCUSSIONS

We carried out  $SU(3)$  lattice gauge simulations in the quenched approximation to calculate the instantaneous color-Coulomb  $q\bar{q}$  potential in the confinement and deconfinement phases. The lattice gauge configurations were generated by the standard heat-bath Monte Carlo technique with a simple plaquette Wilson gauge action.

##### A. Linearity of instantaneous color-Coulomb potential

An example of the variation of the instantaneous color-Coulomb potential  $V(R, 0)$  with distances is shown in Fig. 1, which demonstrates that the potential  $V(R, 0)$  behaves as a linearly rising function with increasing distance  $R$  and can be described in terms of the Coulomb term plus linear term with a nonzero string tension,

$$V(R, 0) = c_0 + KR + e/R, \quad (12)$$

where  $e$  is fixed to  $-\pi/12$  for a two-parameter fit, and  $K = \sigma_c a^2$  is the color-Coulomb string tension. Thus we find that the instantaneous potential  $V(R, 0)$  is a confining potential. In contrast, the vacuum polarization (retarded) part causes color screening, which weakens the confining force as reported in Refs. [11, 13]. Consequently, the color-Coulomb potential in the limit  $n_t \rightarrow \infty$  is expected to approach the Wilson loop potential. The slope of the

potential  $V(R, n_t)$  with finite  $n_t$  decreases as displayed in Fig. 1. Note that the numerical result in Fig. 1 was obtained in the previous work [13], and in the present study, we will not enter into details on the vacuum polarization part any further.

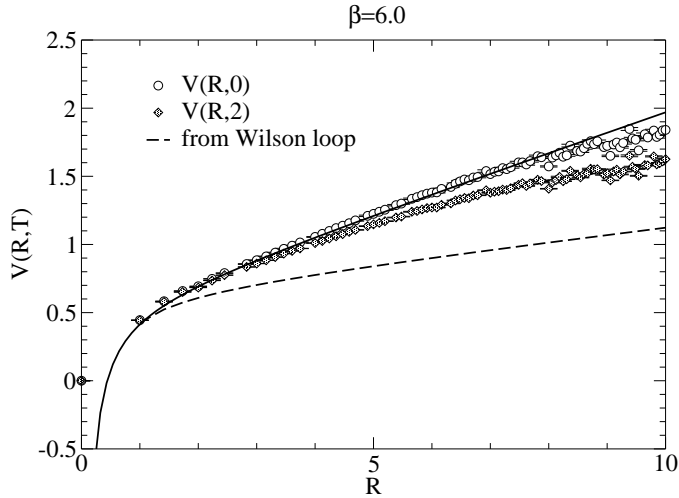


FIG. 1: An example of the  $R$ -dependence of the instantaneous color-Coulomb potential (in dimensionless lattice units) at  $\beta = 6.0$  ( $a \sim 0.1$  fm) on a  $18^3 \times 32$  lattice in the confinement phase. This result was obtained in the previous work [13]. The solid and dashed curves stand for the fitted result for the potential  $V(R, 0)$  and the Wilson loop potential reported in Ref. [16], respectively.

## B. Color-Coulomb string tension

The string tension is a characteristic quantity in discussing confinement physics and thus one should investigate the scaling behavior of the color-Coulomb string tension  $\sqrt{\sigma_c} = \sqrt{K}a^{-1}$ , obtained by the lattice simulation with a finite cutoff. Here we can introduce a two-loop asymptotic scaling of QCD with the mass parameter  $\Lambda$  and lattice cutoff  $a$  as

$$a\Lambda = \exp\left(-\frac{1}{2b_0g^2}\right) (b_0g^2)^{-\frac{b_1}{2b_0^2}} = f(g), \quad (13)$$

where  $b_0$  and  $b_1$  are universal first two coefficients of  $\beta$  function. Since the quantity  $\sqrt{\sigma_c}$  is expected to be proportional to the scale of QCD  $\Lambda$  in asymptotic regions, it makes sense to consider the following relation:

$$\frac{\sqrt{\sigma_c}}{\Lambda} = \frac{\sqrt{K}}{f(g)}, \quad (14)$$

which would be reduced to a constant in the continuum (weak coupling) limit.

In the present study, we carried out calculations at  $\beta = 6.1 - 6.4$  on a  $18^4$  lattice and used 300 gauge configurations measured every 100 sweeps after sufficient thermalization. The  $\beta = 6/g^2$  dependence of the color-Coulomb string tensions is plotted in Fig. 2, in which we additionally employed the data at  $\beta = 5.85 - 6.00$  reported in the previous calculation [13]. For the two-parameter fitting by Eq. (12), we employed the data over  $\mathcal{R} \sim 0.2$  fm up to  $\mathcal{R} \sim 0.5$  fm for  $\beta = 6.1 - 6.4$ , which are  $R \sim 3 - 6$  in lattice units, restricted due to the periodic boundary condition. Although the results of the high  $\beta$  regions have large errors in our calculations [47], the variations of the color-Coulomb string tensions as  $\beta$  varies seem to be smaller than the case of the Wilson loop string tension ( $\sqrt{\sigma_w}$ ) [35], included for comparison. The relative fluctuation (the ratio of the minimum and maximum) of those data is within  $\sim 6(2)$  %. Such tendency was also observed in the  $SU(2)$  lattice simulations [12].

Moreover, in the range of  $\beta$  used here, the value of  $\sqrt{\sigma_c}$  still remains approximately 2 times as large as that of  $\sqrt{\sigma_w}$ , and monotonically varies with  $\beta$ . This tendency seems to be unchanged in the continuum limit. However, the larger lattice simulation at higher  $\beta$  is required to realize the asymptotic scaling.

### C. Behavior of instantaneous color-Coulomb potential at $T \neq 0$

In the confinement phase, as seen in the previous section, the instantaneous color-Coulomb part gives a confining potential. However, it is reported in Refs. [12, 13] that the linearity of  $V(R, 0)$  is not lost even after the QGP phase transition. Therefore, in the present work, we carried out lattice simulations at  $T/T_c = 1.5 - 5.0$  on the fixed lattice size  $24^3 \times 6$ . Here, the critical temperature of the QGP phase transition  $T_c$  is approximately 256 MeV for  $N_t = 6$  [14]. We fixed the lattice temperature  $T = 1/N_t a$  to vary the lattice cutoff  $a$  ( $\beta$ ) [15] and 300 gauge configurations measured every 100 sweeps were used. In Fig. 3, we show the temperature dependence of the *thermal* color-Coulomb potential with a nonvanishing string tension. The potentials  $V(R, 0)$  in the deconfinement phase still behave like a linear-confining potential, and furthermore the slope and magnitude of those potentials become larger. It is found in Fig. 4 that the main temperature dependence of the *thermal*



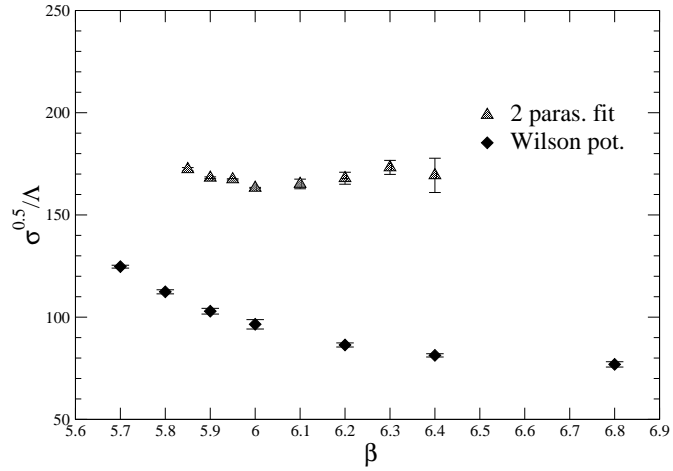


FIG. 2: The dependence of the color-Coulomb string tensions on  $\beta = 6/g^2$ . The triangle symbols with error bar stand for the color-Coulomb string tension in the deconfinement phase. The Wilson loop string tensions, represented by the symbols of the diamond shape, are also plotted for comparison taken from Table III in Ref. [35].

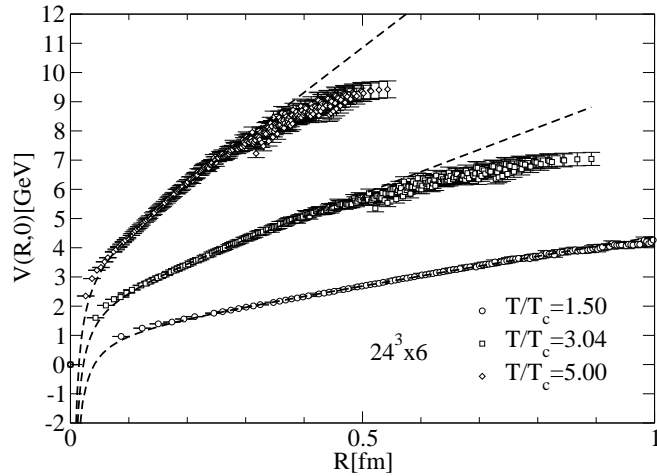


FIG. 3: The dependence of the instantaneous color-Coulomb potential on the temperature in the deconfinement phase. The dashed curves stand for the fitted results.

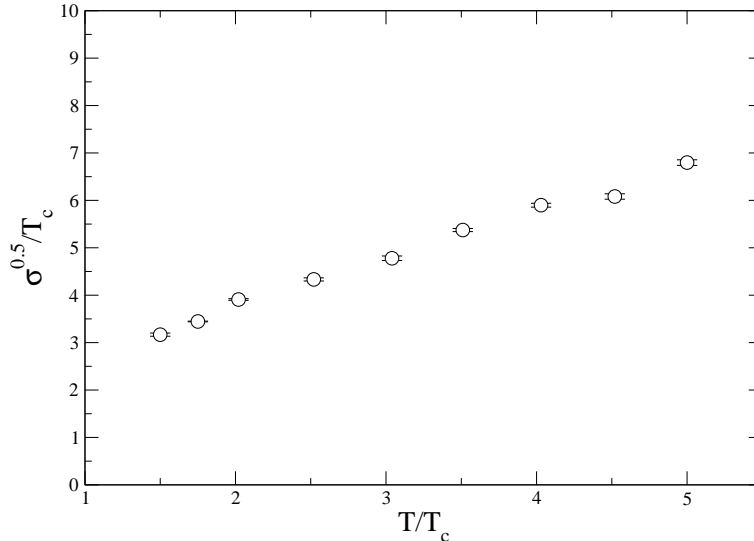


FIG. 4: The temperature dependence of the color-Coulomb string tension in units of  $T_c$  in the deconfinement phase. The color-Coulomb string tension is proportional to  $T$ .

color-Coulomb string tension is apparently given by the linear relation,

$$\sqrt{\sigma_c} \sim T, \quad (15)$$

being directly proportional to the temperature.

#### D. Spatial Wilson loop potential and magnetic scaling

In order to interpret the confining phenomenon caused by the instantaneous color-Coulomb part in the deconfinement phase, it may be instructive to review studies on the thermal behavior of the *spatial* Wilson loop above  $T_c$  [17, 18, 19, 20, 21, 22, 23, 24]. The spatial Wilson loop,  $W(R, S)$ , is constructed by the only spatial links (or spatial gluon fields), where  $R$  and  $S$  are spatial extents on a lattice. If the loop  $W(R, S)$  follows area law as a function of  $S$ , then the spatial Wilson loop potential  $V_s(R)$  would be given by

$$V_s(R) = \lim_{S \rightarrow \infty} \ln \frac{W(R, S)}{W(R, S+1)}. \quad (16)$$

The potential  $V_s$  on the confined  $T = 0$  (symmetric hypercube) lattices can be identical with the usual Wilson loop potential. However, in the deconfinement phase, it is known that the potential  $V_s$  is a linearly rising potential at large distances rather than a color-

screened potential. Consequently, the nonvanishing spatial string tension,  $\sqrt{\sigma_s}$ , exists even in the deconfinement phase.

In a series of studies on the thermal spatial Wilson loop, the spatial string tension  $\sqrt{\sigma_s}$  at high temperature has been discussed in terms of the magnetic scaling. According to perturbation theory of thermal QCD (TQCD) [36], the temporal gluon propagator yields the electric mass,

$$m_e \sim g(T)T, \quad (17)$$

usually referred to as a color-Debye screening mass, while the spatial gluon propagator also yields the magnetic mass

$$m_m \sim g^2(T)T, \quad (18)$$

which must be introduced as the cutoff factor to solve an infrared divergence that appears in TQCD perturbation. Thus, the magnetic scaling somewhat has a nonperturbative origin and is closely relevant to longer range physics than the electric scale.

The infrared sensitivity in TQCD is known to survive in the high temperature limit ( $T \rightarrow \infty$ ) through the argument of 3-dimensional reduction [38, 39]. This approach enables us to obtain the effective theory that is defined by integrating out a nondynamical heavy mode in the high temperature limit; this theory proves that the long-range properties of TQCD are dominated by the magnetic scaling.

### E. Thermal color-Coulomb string tension

To obtain the thermal color-Coulomb string tension  $\sqrt{\sigma_c(T)}$  for the deconfining phase, we employed an ansatz of the Coulomb plus linear terms. The actual fitting analyses by the use of the same function as Eq. (12) give  $\chi^2/ndf \lesssim 1$  for the data of the fixed range of  $R = 3 - 7$  for  $T/T_c = 1.50 - 5.00$ . The thermal color-Coulomb string tensions do not vanish for those temperatures, the values of which increase with temperature, and the rate of increase of the temperature is more rapid than those of the string tension  $\sqrt{\sigma_c(T)}$ . This tendency is acceptable if the color-Coulomb string tension at finite temperature is regarded as a thermal quantity, such as the electric and magnetic scaling described in Eqs. (17) and (18).

From Eq. (4), it is clear that the instantaneous part made by the Faddeev-Popov matrix is independent of time and a spatial-like quantity although the temporal and spatial gluon

fields are correlated by the self-interaction in QCD. This situation is very similar to the case of the spatial Wilson loop at finite temperature as reviewed in the previous section. Therefore, we shall describe these data by the magnetic scaling:

$$\frac{T}{\sqrt{\sigma_c(T)}} = \frac{1}{c} \frac{1}{g^2(T)}, \quad (19)$$

and the running coupling depending on the system temperature,

$$\frac{1}{g^2(T)} = 2b_0 \ln \frac{T}{\Lambda} + \frac{b_1}{b_0} \ln(2 \ln \frac{T}{\Lambda}), \quad (20)$$

where  $c$  and  $\Lambda$  are free parameters for fitting. Using the data for  $T/T_c = 1.5 - 5.0$  we obtained the fitted result, listed in TABLE I, and in particular, the fitted line using the data for  $T/T_c = 2.0 - 4.0$  is shown as the solid line in Fig. 5. It is found that the color-Coulomb string tension in the thermal phase is described by the magnetic scaling.

The fitted results in the present lattice simulation seem to depend significantly on the fitting condition. However, the fitted value of the coefficient by the magnetic scaling is comparable with that reported by the following studies:  $c = 0.566(13)$  and  $\Lambda/T_c = 0.104(9)$  by the lattice calculation of the spatial Wilson loop in Ref. [22],  $c = 0.554(04)$  by the numerical study of the 3-D  $SU(3)$  gauge theory in Ref. [24], and  $c = 0.482(31) - 0.549(16)$  from the lattice calculation of the spatial gluon propagator in Ref. [37]. Furthermore, the analysis of the magnetic mass in a self-consistent way of high QCD theory leads to  $c \sim 0.569$  [40]. If one requires more precise data for magnetic (spatial) or long-range quantities, which are expected to be sensitive to the volume size [37], then the computation on the larger lattice is necessary.

In addition, if we assume the electric scaling given by Eq. (17) to describe the thermal color-Coulomb string tension, then the function  $1/cg(T)$  is employed. The results are listed in TABLE I and the resultant line obtained in the fitted range of  $T/T_c = 2.0 - 4.0$  is shown as the dashed line in Fig. 5. It seems that the electric scaling also yields a good description. In the perturbation theory of the leading order, the coefficient of the electric scaling is known to be  $c = 1$  [36], and moreover the nonperturbative lattice simulation gives the electric scaling with  $c > 1$  [37]. Thus, this procedure may not be as proper a way as the analysis based on magnetic scaling. Nonetheless, this implies that in the temperature range of  $T/T_c = 1.5 - 5.0$ , the magnitude of the coupling constant is of order 1, i.e. there still remains a strong nonperturbative effect. As a result, the distinction between  $g^2(T)$  and  $g(T)$  is not so clear from the present numerical data.

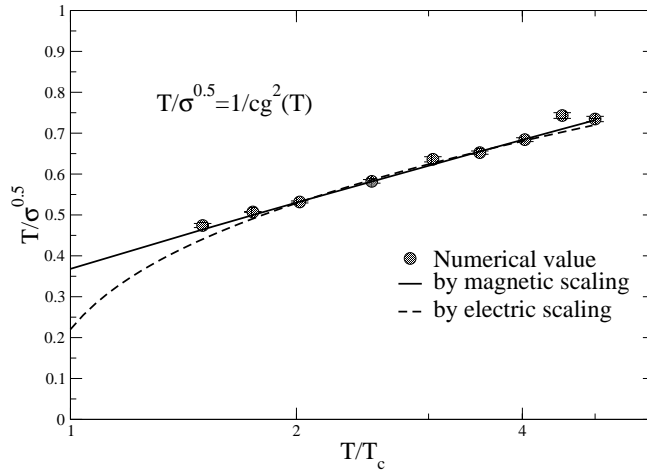


FIG. 5: The dependence of the color-Coulomb string tension as a function of  $T/T_c$ . The circle symbols are numerical data and the solid line represents the fitted result by the magnetic scaling, while the dashed curve (line) represents that by the electric scaling.

## V. CONCLUSIONS

We have investigated the scaling behavior of the color-Coulomb string tension in the confinement and deconfinement phases using quenched  $SU(3)$  lattice gauge simulations. The color-Coulomb potential, defined by the Faddeev-Popov operator, is an important quantity in discussing the confinement scenario in Coulomb gauge, and also from a phenomenological point of view. We have confirmed the scaling behavior of the instantaneous color-Coulomb string tension in the confinement and deconfinement phases.

In the confinement phase, the instantaneous color-Coulomb potential behaves as a linearly rising potential at large distances. As a consequence, there exists the nonvanishing color-Coulomb string tension for several coupling constants ( $\beta$ 's) investigated in this work, the values of which are approximately 2 times as large as that of the Wilson loop string tensions. The variation of color-Coulomb string tension on the lattice cutoff is also found to be small although we are still far from the continuum limit. These results are qualitatively consistent with those obtained by the same analysis in the  $SU(2)$  lattice calculations in Refs. [11, 12]. Note that if one employs the gluon propagator itself to extract the instantaneous part, then

TABLE I: The status on the fitting analyses of the color-Coulomb string tension at  $T \neq 0$ . The second and last rows stand for the fitting range in units of  $T/T_c$  and the value of the reduced chi-square, respectively.

Scaling	Range( $T/T_c$ )	$c$	$T_c/\Lambda$	$\chi^2/ndf$
Magnetic	2.0 - 5.0	0.710(13)	4.05(20)	4.45
	2.0 - 4.0	0.735(18)	4.41(29)	1.47
	1.5 - 4.0	0.770(12)	5.05(20)	1.99
Electric	2.0 - 5.0	0.806(07)	1.36(3)	6.30
	2.0 - 4.0	0.829(10)	1.44(4)	1.25
	1.5 - 4.0	0.869(07)	1.66(3)	5.52

the value of the color-Coulomb string tension tends to become smaller than that measured by using the Polyakov loop correlator as used in the present work [42]. However, it is concluded in Ref. [43] that the emergence of a large string tension is not ruled out.

Even in the deconfinement phase, it is observed that the color-Coulomb string tension remains finite. This may be an acceptable result because the instantaneous part is constructed in terms of the Faddeev-Popov matrix with the derivative operator for the spatial direction; i.e., the instantaneous part is not sensitive to the system temperature. Nevertheless, we should also note that the thermal fluctuation still produces a color-screened dynamics as has been reported in Ref. [13].

The remarkable feature that the color-Coulomb string tension does not disappear in the deconfinement phase was first shown in the  $SU(2)$  lattice calculation [12] done by Greensite, Olejník and Zwanziger. It is confirmed in the present study that the  $SU(3)$  gauge theory has the same feature, and we investigated extensively the temperature dependence of the color-Coulomb string tension, which is found to be in proportion to the temperature. Note that this issue is supported through the discussion of the remnant symmetry in Coulomb gauge [12, 44].

The occurrence of a confining force in the deconfinement phase was observed in other studies. The existence of the spatial string tension above  $T_c$  is well known. In addition,

as reported in Ref. [23], by the  $SU(2)$  lattice simulation in maximally abelian gauge, the spatial Wilson loop can almost be reproduced by the wrapped monopole loops. In particular, the 3-D reduction arguments support these phenomena. For the case of the Coulomb gauge QCD, the confining linearity in the deconfinement phase is caused by the instantaneous part.

In both confinement and deconfinement phases, there is no qualitative change in the behavior of the instantaneous part. Therefore, it is evident that the color-Coulomb string tension obtained from that potential is not an order parameter for the QGP phase transition.

It is found that the thermal behavior of the color-Coulomb string tension is understood by assuming the magnetic scaling,  $\sim g^2(T)T$ , which is actually identified as an infrared regulator or a pole mass of the spatial gluon propagator. If this is a possible interpretation, then we can mention the following two points. Firstly, we conclude that the color-Coulomb string tension in the deconfinement phase is a kind of the thermal quantity and survives in the high temperature limit as being the same as the case of the spatial Wilson loop. Secondly, because the magnetic scaling originates in the infrared sensitivity of the thermal QCD, in the case of Coulomb gauge, the instantaneous part of the gluon propagators reveals such infrared behavior.

In the Coulomb gauge confinement scenario discussed by Gribov and Zwanziger [4, 5], the linearity of the instantaneous part for large quark separations is conjectured to be ascribed to a singularity emerging from the gauge configurations with a low-lying eigenvalue of the Faddeev-Popov operator. Hence, it is an important task that the distribution of the eigenvalues of the Faddeev-Popov operator in Coulomb gauge is investigated by the lattice simulation. The  $SU(2)$  lattice simulation in Coulomb gauge performed in Ref. [41] proves the indication of the enhancement of the low-lying eigenvalues. The  $SU(3)$  lattice study along this line is also being undertaken.

In the present work, we focused the calculation of the instantaneous part only and did not deal with the vacuum polarization (retarded) part, being of little significance in the view of understanding color confinement in Coulomb gauge. However, the vital change concerning the QGP phase transition seems to be relevant to the vacuum polarization part, the role of which ought to be discussed in a subsequent study.

In a phenomenological point of view, it is interesting that there remains the thermal string tension. If this is regarded as the indication that confining features survive above the critical temperature, then this observation may provide some insight into understanding the

strongly correlated QGP. It has been tried in Ref. [45] the description of equation of state in the quasiparticle model with the dispersion relation of Gribov type. However, in other cases, it is not obvious how the confining property in the thermal phase affects physical spectroscopy. Nevertheless, in Coulomb gauge, it is significant that these findings are achieved by classifying the time-time gluon propagator into the instantaneous and noninstantaneous parts.

## VI. ACKNOWLEDGMENTS

The simulation was performed on an SX-5(NEC) vector-parallel computer at the RCNP of Osaka University. We appreciate the warm hospitality and support of the RCNP administrators. This work is supported by Grants-in-Aid for Scientific Research from Monbu-Kagaku-sho (Nos. 13135216 and 17340080).

- 
- [1] H. Toki and H. Suganuma, *Prog. Part. Nucl. Phys.* 45 (2000) S397-S472; H. Toki, *Prog. Theor. Phys. Suppl.* 131, 257 (1998).
  - [2] A. Nakamura and S. Sakai, *Prog. Theor. Phys. Suppl.* 131, 585 (1998).
  - [3] J. Greensite, *Prog. Part. Nucl. Phys.* 51, 1 (2003).
  - [4] V. N. Gribov, *Nucl. Phys. B*139, 1 (1978).
  - [5] D. Zwanziger, *Nucl. Phys. B* 518 (1998) 237-272.
  - [6] L. Baulieu, D. Zwanziger, *Nucl. Phys. B*548 (1999) 527-562, arXiv:hep-th/9807024.
  - [7] A. Cucchieri and D. Zwanziger, *Phys. Rev. D*65 (2002) 014002, arXiv:hep-th/0008248.
  - [8] D. Zwanziger, *Prog. Theor. Phys. Suppl.* 131, 233 (1988).
  - [9] A. Cucchieri and D. Zwanziger, *Phys. Rev. D*65 (2002) 014001, arXiv:hep-lat/0008026.
  - [10] D. Zwanziger, *Phys. Rev. Lett.* 90 (2003) 102001, arXiv:hep-lat/0209105.
  - [11] J. Greensite and Š. Olejník, *Phys. Rev. D*67, 094503 (2003), arXiv:hep-lat/0302018.
  - [12] J. Greensite, Š. Olejník and D. Zwanziger, *Phys. Rev. D*69, 074506(2004), arXiv:hep-lat/0401003.
  - [13] A. Nakamura and T. Saito, *Prog. Theor. Phys.* 115 (2006) 189-200, arXiv:hep-lat/0512042; T. Saito, H. Toki, Y. Nakagawa, A. Nakamura, *Proc. Sci. LAT2005:303,2005*



- [14] G. Boyd, et al., Phys. Rev. Lett. **75**, 4169 (1995).
- [15] K. Akemi, et al., QCDTARO Collaboration, Phys. Rev. Lett. 71 (1993) 3063, hep-lat/9307004.
- [16] G. S. Bali, K. Schilling, Phys. Rev. D47 (1993) 661-672, arXiv:hep-lat/9208028.
- [17] E. Manousakis and J. Polonyi, Phys. Rev. Lett. 58 (1987) 847-850.
- [18] L. Kärkkäinen, et al., Phys. Lett. B312 (1993) 173-178.
- [19] M. Teper, Phys. Lett. B311 (1993) 223-229.
- [20] G. S. Bali, et al., Phys. Rev. Lett. 71 (1993) 3059-3062.
- [21] M. Caselle, et al., Nucl. Phys. B422 (1994) 397-414.
- [22] G. Boyd, et al., Nucl. Phys. B469 (1996) 419-444.
- [23] S. Ejiri, Phys. Lett. B376 (1996) 163-168.
- [24] F. Karsch, et al., Phys. Lett. B346 (1995) 94-98.
- [25] A. Nakamura and T. Saito, Prog.Theor.Phys. 112 (2004) 183-188, arXiv:hep-lat/0406038.
- [26] A. Nakamura and T. Saito, Prog.Theor.Phys. 111 (2004) 733-743, arXiv:hep-lat/0404002.
- [27] H. Reinhardt and C. Feuchter, Phys. Rev. D71, 105002 (2005).
- [28] C. Feuchter and H. Reinhardt, Phys. Rev. D70, 105021 (2004).
- [29] A. P. Szczepaniak and E. S. Swanson, Phys. Rev. D65, 025012 (2002).
- [30] A. P. Szczepaniak, Phys. Rev. D69, 074031 (2004).
- [31] R. Alkofer, M. Kloker, A. Krassnigg, and R. F. Wagenbrunn, arXiv:hep-ph/0510028.
- [32] N. Ligterink and E. S. Swanson, Phys. Rev. C69, 025204 (2004).
- [33] P. O. Bowman and A. P. Szczepaniak, Phys. Rev. D70, 016002 (2004).
- [34] J.E. Mandula and M. Ogilvie, Phys. Lett. B185 (1987) 127.
- [35] G. S. Bali and K. Schilling, Phys. Rev. D47 (1993), 661.
- [36] M. L. Bellac, *Thermal Field Theory* (Cambridge Monographs on Mathematical Physics, Cambridge University Press).
- [37] A. Nakamura, T. Saito and S. Sakai, Phys. Rev. D69 (2004) 014506, arXiv:hep-lat/0311024;  
A. Nakamura, I. Pushkina, T. Saito and S. Sakai, Phys. Lett. B549 (2002) 133-138, arXiv:hep-lat/0208075.
- [38] T. Appelquist and J. Carazzone, Phys. Rev. D11 (1975) 2856.
- [39] T. Appelquist and R. D. Pisarski, Phys. Rev. D23 (1981) 2305.
- [40] G. Alexanian, V.P. Nair, Phys. Lett. B352 (1995) 435-439.
- [41] J. Greensite, Š. Olejník and D. Zwanziger, JHEP 0505 (2005) 070, arXiv:hep-lat/0407032.

- [42] A. Cucchieri and D. Zwanziger, Nucl. Phys. B(Proc. Suppl.) 119(2003) 727.
- [43] K. Langfeld and L. Moyaerts, Phys. Rev. D70 (2004) 074507.
- [44] E. Marinari, M. L. Paciello, G. Parisi and B. Taglienti, Phys. Lett. **B298** (1993), 400.
- [45] D. Zwanziger, Phys. Rev. Lett. 94, 182301 (2005).
- [46] Here, we adopt  $\omega = e^{i\alpha\partial_i A_i}$  as the gauge rotation matrix and suitably chose the parameter  $\alpha$ , which depends mainly on the lattice size.
- [47] We also attempted a 3-parameter fit to Eq. (12), keeping  $e$  as a fitting parameter. However we have not plotted the result of the fit because of the large uncertainty, particularly at high  $\beta$ .